Direct Measurement of Orientation Correlations: Observation of the Landau-Peierls Divergence in a Freely Suspended Tilted Smectic Film

David H. Van Winkle and Noel A. Clark
Department of Physics, Condensed Matter Laboratory, University of Colorado, Boulder, Colorado 80309
(Received 4 June 1984)

Cross-correlation intensity-fluctuation spectroscopy is used to exhibit the space-time behavior of fluctuations in the director orientation difference between a pair of points in the two-dimensional nematiclike director field of a freely suspended tilted smectic film. The Landau-Peierls divergence expected with increasing time is observed directly.

PACS numbers: 61.30.−v, 64.70.Ew, 68.15.+e

The study of the space-time behavior of spontaneous fluctuations in condensed-phase systems has generally been carried out in reciprocal space, with inelastic scattering techniques used to probe fluctuations of some chosen wave vector $\vec{q}$. In this Letter we demonstrate the direct real-space observation of fluctuation dynamics, measuring the cross correlation of orientation at two distinct space-time points of a thermally excited vector field. We exhibit the Landau-Peierls divergence in orientational order in this two-dimensional nematic.

Films, freely suspended in air, an integral number of smectic layers thick may be formed from smectic liquid-crystal phases.[1,2] Certain smectic phases have the average molecular long-axis direction [director $\hat{n}(\vec{r})$] tilted with respect to the layer and film normal, $\hat{z}$. The projection of this director onto the (x,y) plane of the film defines the c director, a unit vector field, $\hat{c}(\vec{r},t)$ completely characterized by its orientation about $\hat{z}$, $\phi(\vec{r},t)$. Depolarized reflection microscopy[3] is used to study the local average orientation $\hat{C}(x,y,t)=\int dz\,\hat{c}(x,y,z,t)$ and $\Phi(x,y,t)=\int dz\,\phi(x,y,z,t)$, variables which define a polar vector field in two spatial dimensions (2D). The static and dynamic properties of $\Phi(x,y,t)$ should be describable using the results of de Gennes, obtained for a hypothetical 2D nonpolar nematic on a liquid surface.[4] Below the Kosterlitz-Thouless transition[2,5] in this system the principal thermal excitations are spin waves and continuous director splay (elastic constant $=K_S$) and bend (elastic constant $=K_B$) orientation fluctuations. If we take the splay and bend elastic constants to be equal, $K=K_S=K_B$ (one-constant approximation), the free energy of fluctuations in Φ is just that of the 2D XY model,

$$F=\frac{K}{2}\int dx\,dy\,(\nabla\Phi)^2=\sum_q\frac{Kq^2}{2}|\Phi_q|^2, \tag{1}$$

where $\Phi_q(t)$ are the Fourier components of $\Phi(x,y,t)$. The dynamics of Φ are well described by simple diffusional relaxation,[1,2] with a correlation function

$$\langle\Phi_q(0)\Phi_q(\tau)\rangle=\langle|\Phi_q|^2\rangle\exp(-Dq^2\tau)=\frac{k_BT}{Kq^2}\exp(-Dq^2\tau). \tag{2}$$

Of primary interest for the experiments reported here is $\sigma(\vec{\rho},\tau)\equiv\langle|\Phi(\vec{\rho},\tau)-\Phi(0,0)|^2\rangle$, the mean square orientation difference for a pair of points separated in space and time by $\vec{\rho},\tau$, which may be written by use of Eq. (2) as

$$\sigma^2(\vec{\rho},\tau)=\frac{2k_BT}{K}\int\frac{d^2q}{4\pi^2q^2}\{1-\exp(i\vec{q}\cdot\vec{\rho})\exp(-Dq^2\tau)\}=\frac{k_BT}{\pi K}\left\{\ln\frac{\rho}{a}+\frac{1}{2}E_1\left(\frac{\rho^2}{4D\tau}\right)\right\}, \tag{3}$$

where E_1 is the exponential integral,[6] $E_1(x)=\int_x^\infty(du/u)\exp(-u)$, and a is a molecular length. $\sigma^2(\vec{\rho},\tau)$ is a monotonic function of time, having zero time derivative at $\tau=0$ and increasing as $\ln(\tau)$ for $\tau>10\tau_c=10\rho^2/4D$. The asymptotic logarithmic increase of σ^2 as $\ln(\rho)$ and $\ln(\tau)$ is the signature of the Landau-Peierls divergence[7] in the 2D XY model and 2D nematics. The orientation field below the Kosterlitz-Thouless transition should thus possess only quasi long-range order (QLRO regime).

The experimental arrangement is shown in Fig. 1. A freely suspended liquid-crystal film of racemic p-decyloxybenzylidene p'-amino 2-methylbutylcinnamate (DOBAMBC)[8] in its smectic-C phase is drawn across a hole of diameter $d=3.2$ mm in a 0.15-mm-thick glass slide. Measurements are presented for a film five

layers thick as determined by optical reflectivity. A 1-mm-diam region on the film is illuminated with convergent polarized light from an argon-ion laser ($\lambda_0 = 4880$ Å). A magnified image ($37\times$) of the film is formed in the reflected light after it passes through a crossed analyzer. The liquid crystal is optically anisotropic, resulting in a slight rotation of the reflected-light polarization vector towards $\hat{C}(x,y)$. Thus, with crossed polarizer and analyzer, the depolarized reflected field is $E(\vec{\rho},\tau) = E_0 \sin[2\Phi(\vec{\rho},\tau)]$.[3] In the magnified film image are positioned two 500-μm-diam optical fibers, which probe the reflected intensity averaged over two 13.5-μm-diam regions on the film. These fibers transmit the reflected light to photomultiplier tubes and equivalent-photon–counting electronics. The resulting photopulse trains $n_1(t)$ and $n_2(t)$ are fed into a digital correlator (Langley-Ford 1096), which computes in real time the cross-correlation function,

$$R(\rho,\tau_n) = \langle n_1(t) n_2(t+\tau_n)\rangle \propto \langle I(0,0) I(\rho,\tau_n)\rangle,$$

for various times τ_n over the total range τ_N ($n \leq N = 136$). We define the quantity $\Xi(\rho,\tau_1,\tau_n) = R(\rho,\tau_1) - R(\rho,\tau_n)$ and show in Fig. 2 measurements of

$$S(\vec{\rho},\tau_n) \equiv \frac{\Xi(\vec{\rho},\tau_1,\tau_n)}{\Xi(\vec{\rho},\tau_1,\tau_N)} = \frac{\langle I(0,0)[I(\vec{\rho},\tau_1) - I(\vec{\rho},\tau_n)]\rangle}{\langle I(0,0)[I(\vec{\rho},\tau_1) - I(\vec{\rho},\tau_N)]\rangle}, \tag{4}$$

for two different mean orientations of $\hat{C}$ relative to $\vec{\rho}$, at changing time scales and for the indicated temperatures. We choose a region in the film plane where $I \approx E_0^2/2$, for which I is nearly linear in Φ. If we take $I(\vec{\rho},\tau) = \alpha\Phi(\vec{\rho},\tau)$, we may replace $I(\vec{\rho},\tau)$ by $\Phi(\vec{\rho},\tau)$ in Eq. (4). It can then be shown that $S(\vec{\rho},\tau_n) \propto \sigma^2(\vec{\rho},\tau_n) - \sigma^2(\vec{\rho},\tau_1)$.

Curves *a–c* of Fig. 2 show $S(\vec{\rho},\tau)$ data for which $\vec{\rho}$ is perpendicular to the averge orientation of $\hat{C}$ ($\chi = \pi/2$). We refer to this as the splay case since the fluctuations probed in this orientation involve predominantly splay of the director. Curves *d–f* of Fig. 2 are data for which $\vec{\rho}$ is parallel to the average orientation of $\hat{C}$ ($\chi = 0$), the bend case. Note the qualitative difference between the splay and bend data (nonmonotonic behavior of the bend data). This difference indicates that it may not be appropriate to ignore the strong elastic anisotropy in this system[2] ($K_B \approx K_S/6$) as has been done up to this point. Furthermore, using separately K_S and K_B extrapolated from the data of Rosenblatt *et al.*[2] for the elastic constant K in Eq. (3), we can estimate for our experiments the root mean square

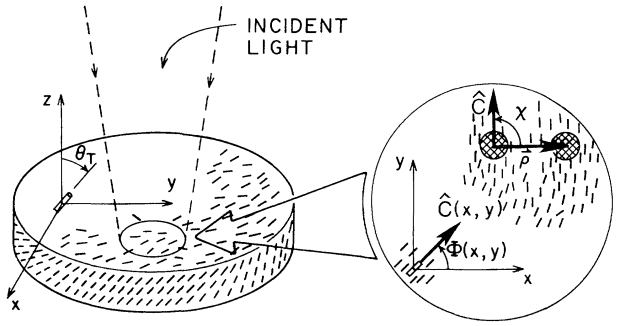

FIG. 1. Freely suspended liquid-crystal film geometry. (a) Structure of a three-layer smectic-*C* film (≈ 75 Å thick) with convergent polarized light illuminating a 500-μm-diam area. The molecules are tilted with respect to the *z* axis an angle θ_T. The average local projection of $n(r)$ onto the film plane defines $\hat{C}(x,y)$. (b) Angular displacement, $\Phi(x,y)$, of $\hat{C}(x,y)$ in the *XY* plane, the film plane. The shaded areas represent the 13.5-μm-diam regions occluded by fiber optic probes, with the splay case illustrated. The intensity of depolarized light collected by each of the probes is sensitive to the average local orientation of $\hat{C}$ over its shaded area. The light from the two probes is analyzed in real time by a digital cross correlator.

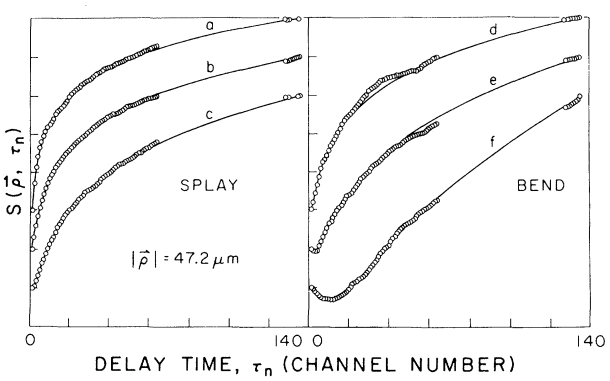

FIG. 2. Plots of $S(\vec{\rho},\tau_n) = \Xi(\vec{\rho},\tau_1,\tau_n)/\Xi(\vec{\rho},\tau_1,\tau_N)$ with $N = 136$. The data are scaled to have the same height from initial to final points. Runs *a*, *b*, and *c* are the splay case at 74.8 °C and are fitted with $D_S = 1.3 \times 10^{-4}$ cm^2/sec. The time delays between first and last data points: curve *a*, 50 sec; curve *b*, 6 sec; and curve *c*, 1.5 sec. Runs *d*, *e*, and *f* are the bend case at 66.5 °C and with $D_B = 1.1 \times 10^{-5}$ cm^2/sec. The first- to last-channel delays: curve *d*, 40 sec; curve *e*, 10 sec; and curve *f*, 2.5 sec. The shorter-time bend runs show the nonmonotonic contribution due to third harmonic coupling fluctuations in Φ to the reflected field.

(rms) orientation difference $\sigma(\vec{\rho},\tau)$ along $\hat{C}$ ($\chi=0°$, bend) and perpendicular to $\hat{C}$ ($\chi=90°$, splay): $\sigma(\vec{\rho},\tau)<7°$ for splay and $\sigma(\vec{\rho},\tau)<20°$ for bend. For the bend case σ is large enough to necessitate inclusion of the next-higher-order terms in the dependence of $E(\vec{\rho},\tau)$ on Φ. The result for $\Xi(\vec{\rho},\tau_1,\tau_n)$ is[9]

$$\Xi(\vec{\rho},\tau_1,\tau_n)=\langle 4\,\delta\Phi(0,0)[\delta\Phi(\vec{\rho},\tau_1)-\delta\Phi(\vec{\rho},\tau_n)] - \tfrac{32}{3}\{\delta\Phi(0,0)[\delta\Phi^3(\vec{\rho},\tau_1)-\delta\Phi^3(\vec{\rho},\tau_n)]+\delta\Phi^3(0,0)[\delta\Phi(\vec{\rho},\tau_1)-\delta\Phi(\vec{\rho},\tau_n)]\}\rangle. \quad (5)$$

For $\chi=0$ or $\pi/2$, pure bend or splay fluctuations dominate $\Xi(\vec{\rho},\tau_1,\tau_n)$, and the data can be analyzed in the one-constant approximation, with an effective diffusion constant, D, appropriate to the geometry. Calculating the thermal averages in the one-constant approximation yields[9]

$$\Xi(\vec{\rho},\tau_1,\tau_n)\propto E_1\left(\frac{\rho^2}{4D\tau_n}\right)-E_1\left(\frac{\rho^2}{4D\tau_1}\right)-A_4\{\ln\frac{\rho}{a}[E_1(2D\tau_1q_m^2)-E_1(2D\tau_nq_m^2)]+\text{smaller terms}\}, \quad (6)$$

where q_m is the minimum wave vector probed and the amplitude of the $\delta\Phi\,\delta\Phi^3$ contribution is $A_4=2k_BT/\sqrt{K_SK_B}$. The first two terms are just those obtained above for $I\propto\Phi$ and the terms multiplied by A_4 are associated with $\delta\Phi\,\delta\Phi^3$ coupling. At any particular temperature D is almost an order of magnitude smaller for the bend case than for the splay case, and since E_1 is a monotonically decreasing function the third-harmonic coupling will be more significant in the bend case. The largest $\delta\Phi\,\delta\Phi^3$ terms involve q_m, and therefore the longest-wavelength fluctuations encountered in the experiment. q_m is either the system size ($q_m=\pi/d\simeq 10$ cm^{-1}) or the smallest-wave-vector fluctuation observable in the experimental run time [$q_m=(\pi^3/Dt_{\text{run}})^{1/2}$], whichever is larger. The nonlinear contributions of the long-wavelength fluctuations in fact dominate at short delay times making $S(\vec{\rho},\tau_n)$ negative. At longer delay times the Landau-Peierls divergence appears and the linear terms dominate the fluctuations, decorrelating the relative orientation, and making S positive and logarithmically increasing.

Using Eq. (6) we obtain good fits to both the splay and bend data shown in Fig. 2. Curves a–c of Fig. 2 show $S(\vec{\rho},\tau_n)$ for the splay case for a fixed probe separation ($\rho=47.2$ μm) for three delay-time ranges, respectively $\tau_N=1140\tau_c$, $\tau_N=140\tau_c$, and $\tau_N=35\tau_c$ where $\tau_c=\rho^2/4D_S=4.3\times10^{-2}$ sec is obtained as a fitting parameter. For the splay case the rms fluctuations in Φ are sufficiently small ($\sigma\leq 7°$) that the nonlinearly coupled terms are negligible and the data can be fitted with only the first two terms in Eq. (6). Curves b and c of Fig. 2 exhibit the exponential integral dependence of the decorrelation at short times. For long times $E_1(\tau_c/\tau)\approx\ln(\tau/\tau_c)$ and the normalized correlation function $S(\vec{\rho},\tau_n)$ approaches an asymptotic logarithmic form which is scale invariant (independent of τ_N). This scale-invariant divergence is distinctive of the Landau-Peierls instability. The long time-scale run, Fig. 2, curve a, requires accumulating data for on the order of 4 h to obtain adequate statistical averaging over the $\leq$ 50-sec fluctuations that affect the shape of $S(\vec{\rho},\tau_n)$. Varying the probe separation ρ yields the $\tau_c\propto\rho^2$ scaling, expected for the proposed diffusional dynamics. At small probe spacing, effects due to nonzero probe size appear and are adequately accounted for by including a Gaussian probe profile when calculating the thermal average in Eq. (3).[9]

For the bend case rms fluctuations in Φ are larger than for the splay case, and $\delta\Phi\,\delta\Phi^3$ terms contribute significantly at short times. Curves d–f of

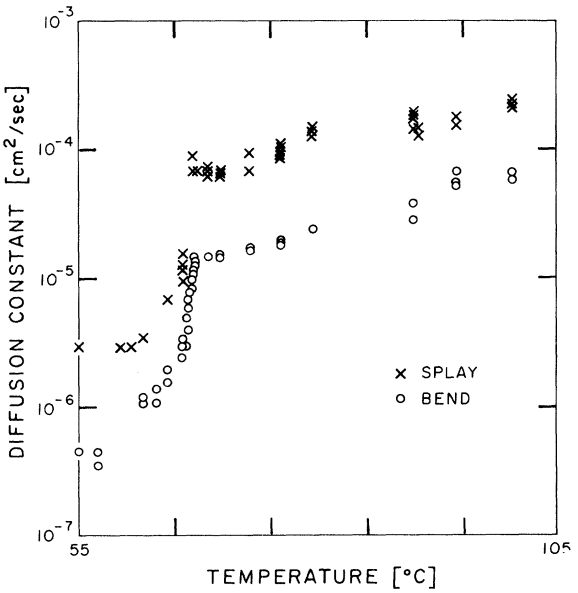

FIG. 3. Plots of experimentally determined orientational diffusion constants $D=K/\eta$ as a function of temperature. The SmC-SmI phase transition is observed as a decrease in both D_S and D_B by a factor of ≈ 6 at 66 °C.

Fig. 2 show $S(\vec{\rho}, \tau_n)$ for the bend case for $\rho = 47.2$ μm and $\tau_N = 78\tau_c$, $19\tau_c$, and $48\tau_c$, respectively, with $\tau_c = \rho^2/4D_B = 5.1 \times 10^{-1}$ sec. Figure 2, curve *f*, shows the contribution of the $\delta\Phi\,\delta\Phi^3$ terms as an initial decrease in $\Xi(\vec{\rho}, \tau_1, \tau_n)$.

The values of D_S and D_B obtained for best fit are consistent with the data of Rosenblatt[2] extrapolated to the temperature used. The value of $A_4 = 2k_BT/\sqrt{K_SK_B}$ obtained was within 25% of that predicted from extrapolation for K_S and K_B. Since τ_c scales as D^{-1} and D_B is observed $\approx D_S/6$, τ_c in the bend case must be a factor of 6 larger than in the splay case for equivalent statistics, making bend data observation at large τ_n difficult; for instance, curve *d* of Fig. 2 is a 12-h run.

Figure 3 shows the temperature dependence of the diffusion constants, with the splay diffusion constant at all temperatures about a factor of 6 larger than the bend diffusion constant. There is a steady decrease in both D_S and D_B with decreasing temperature as the smectic-*C* (Sm*C*) to smectic-*I* (Sm*I*) phase transition is approached. Across the Sm*C*-Sm*I* transition the diffusion constants drop abruptly, and continue to decrease with decreasing temperature inthe Sm*I* phase. This temperature behavior of the diffusion constants may be understood as an increase of the orientational viscosity at a larger rate than the orientational elastic constants as the correlation length for short-range translational ordering in the smectic planes increases with decreasing temperature.

We have demonstrated the use of cross-correlation intensity-fluctuation spectroscopy to directly probe the space-time behavior of fluctuations in a condensed phase, using polarized reflection microscopy to study 2D orientation-fluctuation dynamics in tilted smectic liquid-crystal films at length scales not readily accessible by scattering techniques. We have directly observed the Landau-Peierls divergence expected in this system. We also find important contributions to the observed intensity correlation functions due to cubic terms in the coupling of orientation fluctuations to the probing fields.

This work was supported by the National Science Foundation under Grant No. DMR 83-07157.

[1]C. Y. Young, R. Pindak, N. A. Clark, and R. B. Meyer, Phys. Rev. Lett. **40**, 773 (1978).

[2]C. Rosenblatt, R. B. Meyer, R. Pindak, and N. A. Clark, Phys. Rev. A **21**, 140 (1980).

[3]R. Pindak, C. Y. Young, R. B. Meyer, and N. A. Clark, Phys. Rev. Lett. **45**, 1193 (1980).

[4]P. G. de Gennes, Faraday Symp. No. 5, 1971; and *The Physics of Liquid Crystals* (Oxford, London, 1974), p. 111.

[5]D. R. Nelson and J. M. Kosterlitz, Phys. Rev. Lett. **39**, 1201 (1977).

[6]M. Abramowitz and I. A. Stegun, *Handbook of Mathematical Functions* (Dover, New York, 1972), p. 228.

[7]*Statistical Physics,* Course of Theoretical Physics, edited by L. D. Landau and E. M. Lifshitz, Vol. 5 (Pergamon, New York, 1980), 3rd ed., Part 1, p. 433; R. E. Peierls, Helv. Phys. Acta. **7**, Suppl. 11, 81 (1974).

[8]DOBAMBC (*p*-decyloxybenzylidene-*p'*-amino-2-methylbutylcinnamate) is 2-propenoic acid, 3-[4-[[[4-(decyloxy)phenyl]methylene]amino] phenyl]-2-methylbutyl ester, and has a phase diagram in the five-layer free film

Crystal $\xrightarrow{67\,^\circ\mathrm{C}}$ Smectic-*C* $\xrightarrow{115\,^\circ\mathrm{C}}$ Smectic-*A* ⟷ Isotropic

Smectic-*I* $\swarrow$ 66 °C

[9]D. H. Van Winkle and N. A. Clark, to be published.